FUNCTIONAL POLYMERS

AC Impedance Analysis of Lithium Ion Based PEO:PVP Solid Polymer Blend Electrolytes

K. Sundaramahalingam[a], M. Muthuvinayagam[b],*, and N. Nallamuthu[b]

[a] *Multi-functional Materials Laboratory/International Research Center, Kalasalingam Academy of Research and Education, Krishnankoil, 626 126, Tamilnadu, India*
[b] *Department of Physics/School of Advanced Sciences, Kalasalingam Academy of Research and Education, Krishnankoil, 626 126, Tamilnadu, India*
* e-mail: mmuthuvinayagam@gmail.com

Abstract—Lithium ion conducting poly(ethylene oxide) (PEO):poly(vinyl pyrrolidone) (PVP) polymer blend electrolytes have been prepared by solution casting technique. The XRD and FTIR analysis confirm the complexation between salt and polymers. The conductivity of the samples is analyzed by impedance spectroscopy technique within the frequency range of 42 Hz to 1 MHz in the temperature range of 303 to 363 K. The conductivity of polymer electrolytes increases up to 20 wt % of lithium acetate concentration and the higher conductivity is found to be 2.56×10^{-6} S/cm at room temperature. The transference number measurements are also carried out using Wagner polarization technique.

INTRODUCTION

In the recent years, polymer electrolytes are broadly considered because of their potential electrochemical applications in batteries, energy units, super capacitors, electro-chromic sensors [1]. Polymer electrolytes have numerous points of interest such as adaptability, simplicity of processing into thin films, electrochemical strength and sealing nature [2]. There are few procedures used to prepare polymer electrolytes, for example, blending of polymers [3], copolymerization, addition of plasticizers and ceramic nanofillers [4] to enhance the ionic conductivity of Polymer electrolytes. PEO has both crystalline and amorphous nature at room temperature [5]. In 1972, Wright detailed about the Ionic conductivity of PEO with soluble alkali metal salt complexes [6]. The main short-comings of PEO based solid polymer electrolytes are poor ionic conductivity (10^{-8}–10^{-7} S/cm) at surrounding temperature [7] and low cation transference number (<0.3) [7–10]. As of late, PEO has been easily formed as films and has good lithium ion stability. So that, it has been widely contemplated as an electrolyte and separator materials. The coordination bonds have been formed by wrapping the lithium ion with the polymeric chain of PEO [11, 12].

To improve the amorphous nature and conductivity, the blending of polymers is one of the viable ways. Blending of polymers frequently display improved properties that are better than the single polymer [13]. Among the conjugated polymers, PVP is unique organic one because of its high amorphous nature that allows quicker ionic mobility. The development of various complexes with diverse inorganic salts is possible by using PVP because of the existence of the carbonyl group (C=O) in the side chain. PVP is exceedingly solvable in polar solvents, for example, alcohol, water, etc. And also having high glass transition temperature T_g with great eco-friendly, thermal and mechanical stability [14]. The another preferred point of PVP is that the formation of thermally cross connected polymer chain and accordingly, it has extraordinary thermal stability and high mechanical strength of blend materials [15, 16]. On account of its exceptional attributes, Poly(vinyl pyrrolidone) (PVP) was chosen as another polymer to prepare polymer blends with PEO.

In last couple of years, ion based strong polymer electrolytes have been prepared. Lithium batteries have high energy density because of high polarizing energy of lithium ions and little cationic size. The interesting points like no-spillage of electrolyte, higher energy density, adaptable geometry and enhanced well-being perils attract the researchers to work on lithium polymer batteries [17–19]. In the current work, the solid polymer blend electrolytes based on the PEO/PVP in addition of different ratios of lithium acetate have been prepared by solution casting technique and characterized by various techniques.

EXPERIMENTAL

PEO (Molecular weight 4×10^6 g/mol) is purchased from Aldrich chemicals USA, PVP (molecular weight, $M_w = 9 \times 10^5$) is purchased from (S-d fine chem-Ltd), India and lithium acetate of molecular weight $M_w = 102.02$ is purchased from Merck, India. The solution casting technique is simple and flexible method to prepare polymer electrolyte. Double distilled water is used as solvent. PEO, PVP and lithium acetate are taken in the ratios of (67.5 : 27.5 : 5) (65 : 25 : 10) (62.5 : 22.5 : 15) and (60 : 20 : 20). Initially the polymers PEO, PVP and lithium acetate are dissolved in distilled water separately. Then it is mixed and stirred well. The resultant homogeneous solution is poured into Petri dish and allowed for solvent evaporation.

The Powder X-ray Diffraction pattern of the polymer blend electrolytes is detailed using Bruker make X-Ray diffractometer using Cu $K\alpha$ radiation ($\lambda = 1.540$ Å) with scanning rate 5° per minute in the range of 10°−80°. The FTIR transmittance spectra of the films are detailed using "SHIMADZU IR Tracer 100" Spectrometer with a resolution of 4 cm^{-1} in the wave number range of 400–4000 cm^{-1}. The impedance measurements are done by the computer controlled HIOKI 3532-50 LCR Hi-tester within the frequency range of 42 Hz−1 MHz in the temperature range of 303−363 K. Wagner's polarization technique is used to determine the ionic and electronic transference numbers.

RESULTS AND DISCUSSION

X-Ray Diffraction Studies

X-ray diffraction is a main technique to define the amorphous nature of the blend polymers. Figure 1 displays the X-ray diffraction pattern of various composition of lithium acetate complexed with PEO/PVP polymer electrolytes. The sharp diffraction peaks appeared at 18° and 23° corresponding to PEO indicates the crystalline nature [20]. After blending PVP with PEO, the peak intensity decreases. As increasing the concentration of salt with the polymer blend, the sharp diffraction peaks become, reducing that indicates the increase in amorphous nature in whole polymer system. There is no peak corresponding to lithium acetate were observed that specifies the nonexistence of extra salt in the blend polymer films and the broad dispersion of salt with the polymer system. The characteristic peaks of PEO/PVP/20 wt % lithium acetate have decreased to a maximum amount than the other prepared blend polymers.

FTIR Analysis

FTIR investigation is performed to determine the interaction between the salt and polymers in the electrolytes. The distinctions in the spectral features have been seen on looking at the spectra of PEO/PVP with various concentration of lithium acetate are exhibited. FTIR spectra of different compositions of (PEO/PVP/lithium acetate) are given in Figs. 2a and 2b. It is conceivable to ascribe the transmittance bands of lithium acetate mixed blend polymer complex. The diverse vibrational modes of interaction strengths and the occurrence of specific groups may possibly affirm the presence of different element of the electrolyte films.

The bands appearing at 3500−3000 cm^{-1} demonstrates the OH vibration, the band increases by increasing the concentration of lithium acetate. A peak at 2885 is seen owing to the asymmetric (CH) bending of CH$_2$ of PEO [21]. The band at 1343 cm^{-1} is because of CH$_2$ bending of PEO. The robust interaction in PEO is CH$_2$ twisting at 1282 cm^{-1}, which is moved to 1278 cm^{-1}, may be because of the bonding of CH$_3$COO-Li with PEO/PVP. The slight band at about 1238 cm^{-1} is allotted to CH$_2$ symmetric stretching of PEO [21]. The vibration band at 1099 cm^{-1} is fixed to C−O−C (symmetric and asymmetric) stretching of PEO [23] that is moved somewhat in all the complexes. The mode in charge of the band at 845 cm^{-1} is essentially owing to the CH$_2$-rocking through a slight commitment from C−O stretching movement of PEO while band at 947 cm^{-1} starts fundamentally in the C−O stretching with some CH$_2$-rocking [22].

The vibrational band at 1020 cm^{-1} might be because of the stretching of C−O in PEO. The intensity of the peak increases by increasing the salt concentration. These outcomes form the coordination bonds between Li$^+$ particle and ether units (−O−) of PEO. So that the spectral changes are probable in the C−O−C stretching and deformation ranges. The band around 1463 cm^{-1} are ascribed to C=O stretching and CH$_2$ wagging of PVP of the all complexes respectively. Conversely, for pure PVP, a vibration band observed at 2885 cm^{-1} may possibly be ascribed to aliphatic C−H stretching of PVP [23]. The bands around 1463 cm^{-1} are ascribed to C=O stretching and CH$_2$ wagging of PVP of all complexes respectively. Consequently, the spectral analysis approves the complexation of polymer blend and lithium salt. Table 1 shows the vibrational frequencies of PEO/PVP/lithium acetate polymer electrolytes.

AC Impedance Analysis

The characteristic impedance plots (Z' vs. Z'') for PEO/PVP/X wt % lithium acetate polymer electrolytes at ambient temperature are shown in Fig. 3. There exists a depressed semicircular portion in all the polymer systems. In the complex impedance, representation, by increasing the salt concentration, there exists a spike. The appearance of the spike is mainly because of the typical jamming double-layer capaci-

Intensity, a.u.
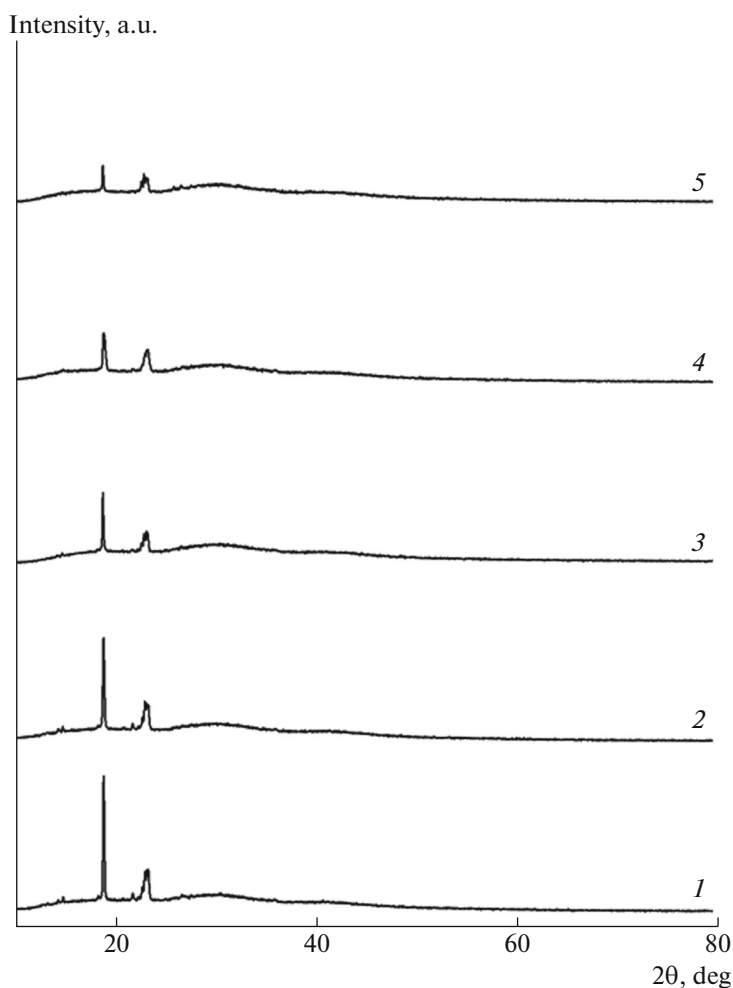
Fig. 1. XRD Pattern of different ratios of lithium acetate doped PEO/PVP polymer systems: (*1*) 0, (*2*) 5, (*3*) 10, (*4*) 15, and (*5*) 20 wt %.

tance. The bulk response of the films in high frequency region is indicated by the semicircle. In the equivalent circuit, the semicircle is noted by the parallel combination of resistance and capacitance and this combination produces the impedance effect due to the passage of ions and the polarization of immobile polymer chains [24].

The intercept of the spike on *X*-axis of the complex impedance plot gives the bulk resistance. The ionic conductivity is calculated by the formula:

$$\sigma = l/R_b A, \qquad (1)$$

where *l*—thickness of the film, *A*—area of the film and R_b—bulk resistance of the material. By increasing the salt concentration, the conductivity increases due to the raise in number of movable charge carriers and a drop in the crystallinity nature of polymer electrolytes. The polymer electrolyte PEO/PVP/20 wt % lithium acetate shows the higher conductivity of 2.56×10^{-6} S/cm. The ionic conductivity demonstrates the effective collaboration among oxygen atoms and Li^+ cations in the

electrolytes [25, 26]. From Fig. 4, it is detected that the conductivity is increasing by increasing the temperature, indicating the raise in amorphous nature of the polymer electrolytes. The polymer electrolytes have more flexible chain that promotes the segmental motion of polymer that encourages higher mobility [27].

Temperature Dependent Conductivity

Figure 5 exhibits the linear dependence of log σT with respect to inverse temperature ($1000/T$) for blend and lithium acetate complexed films. The direct deviation in log σT versus $1000/T$ plot prescribes an Arrhenius-type of thermally started process denoted by

$$\sigma = \sigma_0 \exp(-E_a/KT), \qquad (2)$$

where σ_0 is the pre-exponential factor, E_a—activation energy, *K*—Boltzmann constant and *T*—absolute temperature. In all the compositions of the polymer blend
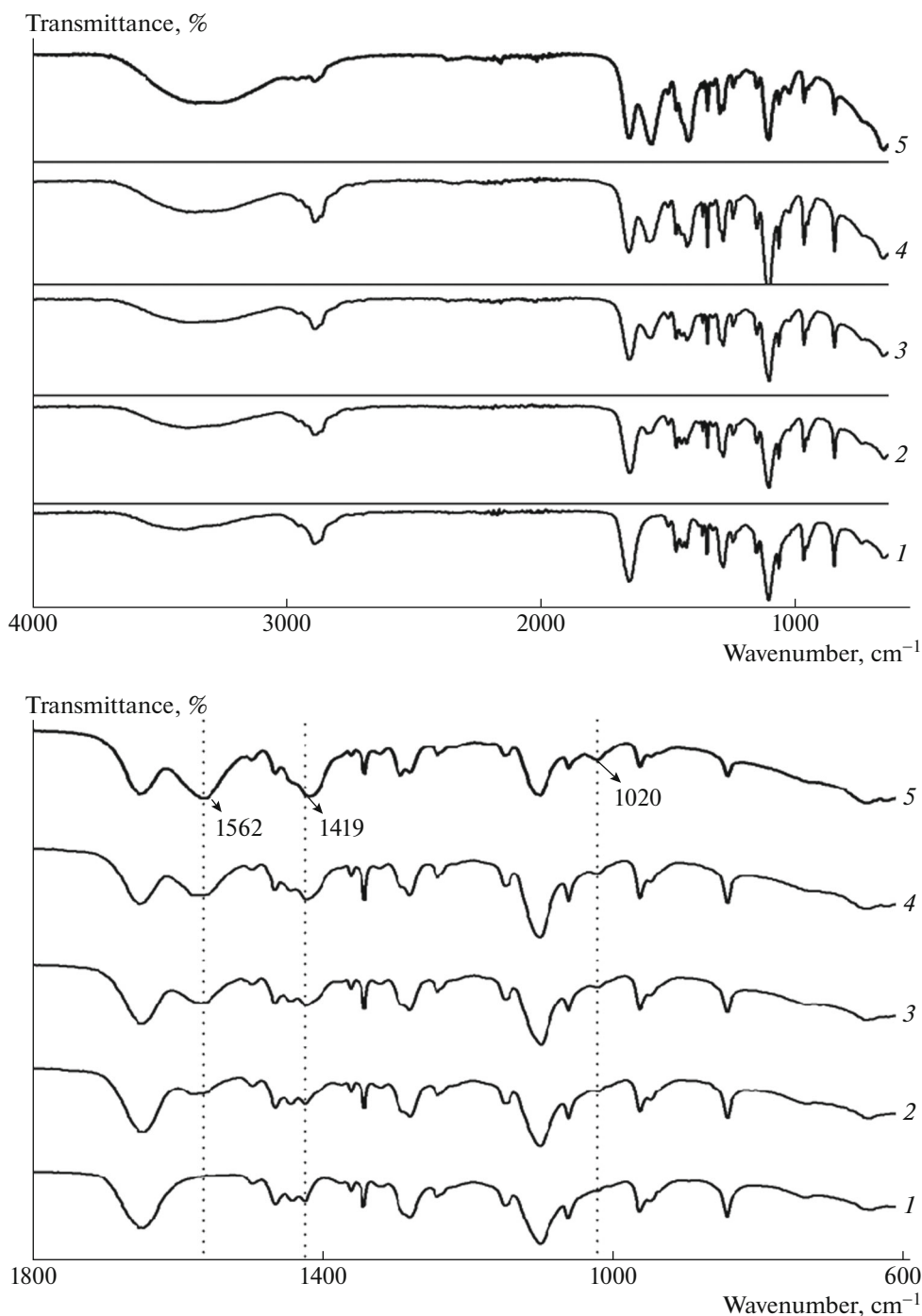
Fig. 2. FTIR spectra of PEO/PVP/lithium acetate blend polymer electrolytes: (*1*) 0, (*2*) 5, (*3*) 10, (*4*) 15, and (*5*) 20 wt %. (a) 4000–600 cm^{-1}, (b) 1800–600 cm^{-1}.

electrolytes, ionic conductivity is found to increase with increase in temperature [28–30].

At the point, when the temperature increases, there is a creation of little measure of space encompassing its specific volume because of the vibrational energy of a fragment of polymer chain. The vibrating energy winds up adequate to thrust against the hydrostatic pressure forced by its nearby atoms in this manner making free volume [31]. In this manner, the free volume all over the polymer chain creates the movement of the ions and the segmental movement of polymer chain and along these builds the conductivity. The expansion in amorphous nature of the polymer blend electrolyte gives a more free volume in the polymer

Table 1. Vibrational frequencies of different concentrations of lithium acetate with PEO : PVP

Vibrational mode	PEO/PVP/ 0 wt % of lithium acetate	PEO/PVP/ 5 wt % of lithium acetate	PEO/PVP/ 10 wt % of lithium acetate	PEO/PVP/ 15 wt % of lithium acetate	PEO/PVP/ 20 wt % of lithium acetate
Symmetric C−H stretching	2885	2887	2885	2885	2887
C−H bending of CH_2	1463	1460	1463	1460	1461
CH bending	1342	1342	1342	1340	1340
C−H second overtone	1278	1280	1278	1280	1278
CH_2 twisting	1238	1238	1238	1238	1238
C−C stretching	1147	1147	1147	1145	1147
Symmetric and asymmetric C−O−C stretching	1099	1099	1099	1101	1099
C−O stretching with some CH_2 asymmetric rocking	957	960	962	956	962
CH_2 rocking in PVP and with some C−O stretching in PEO	842	840	842	840	840

electrolyte framework on expanding temperature [32]. By using the linear fitting of Arrhenius plots, the activation energy values are calculated for the prepared polymer electrolytes and are listed in Table 2. By increasing the concentration of lithium acetate, the value of activation energy is found to be decreased steadily. Figure 6 shows the composition dependent conductivity of polymer electrolytes.
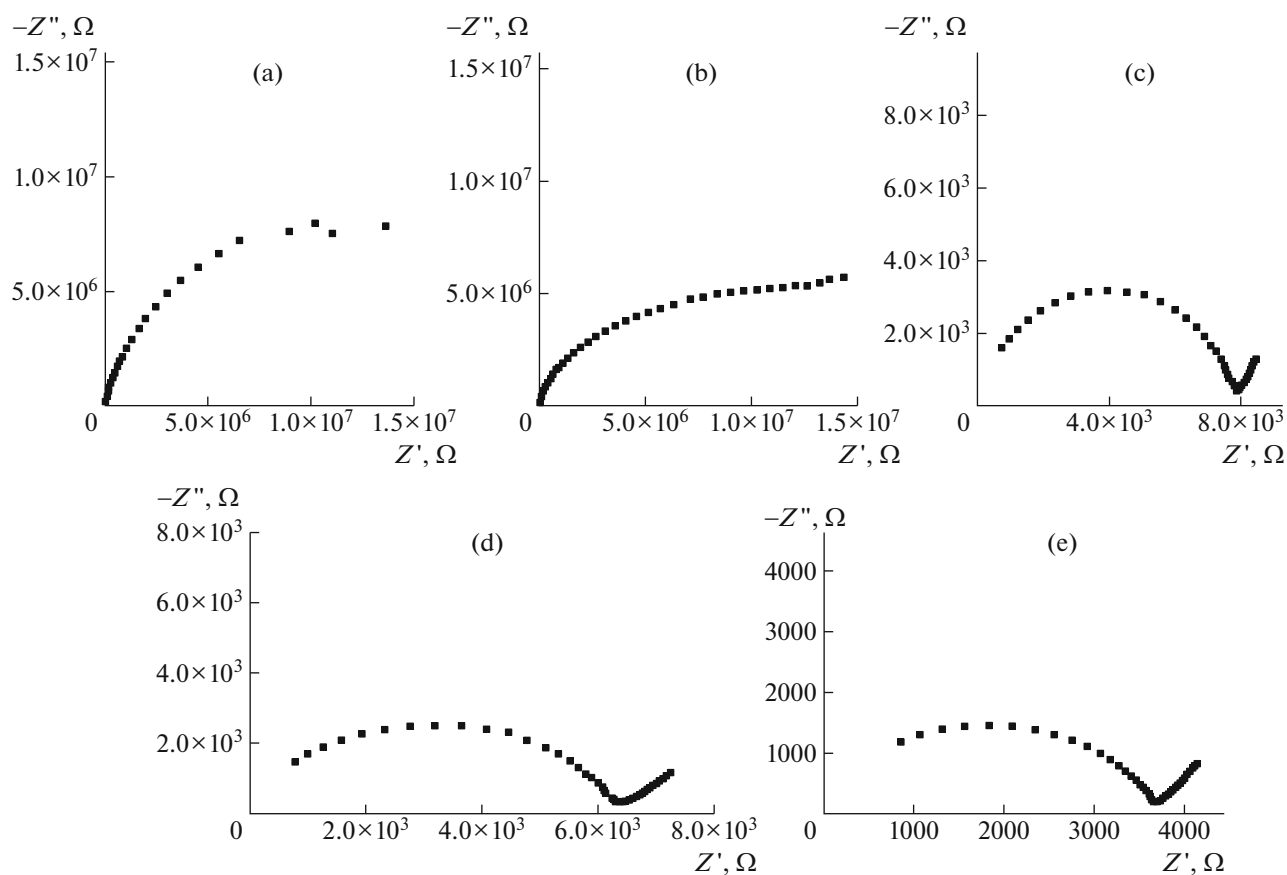
Fig. 3. Cole-Cole plot of different weight percentage of lithium acetate doped with PEO/PVP: (a) 0, (b) 5, (c) 10, (d) 15, and (e) 20 wt %.
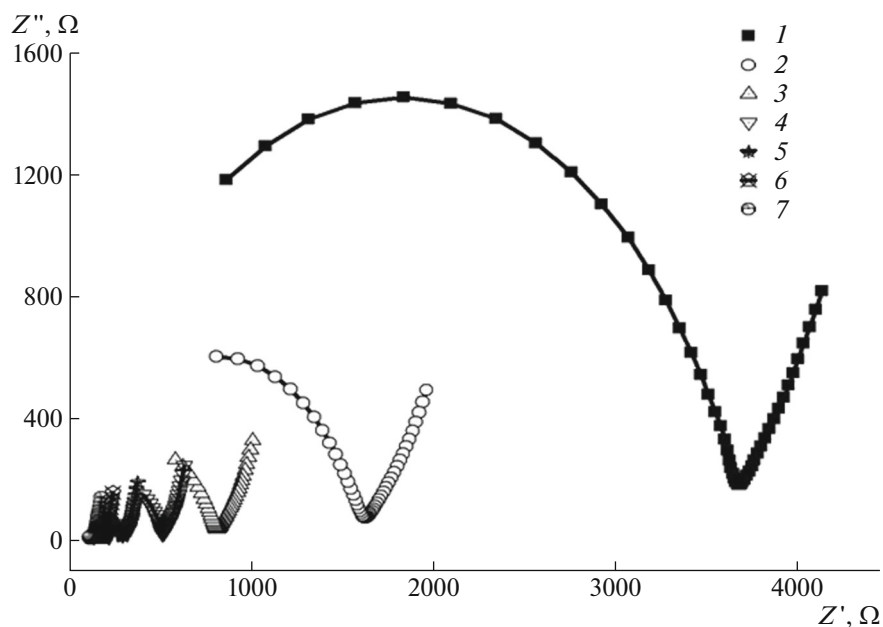
Fig. 4. Cole-Cole plot of PEO/PVP/20 wt % lithium acetate at different temperatures: (*1*) 303, (*2*) 313, (*3*) 323, (*4*) 333, (*5*) 343, (*6*) 353, and (*7*) 363 K.
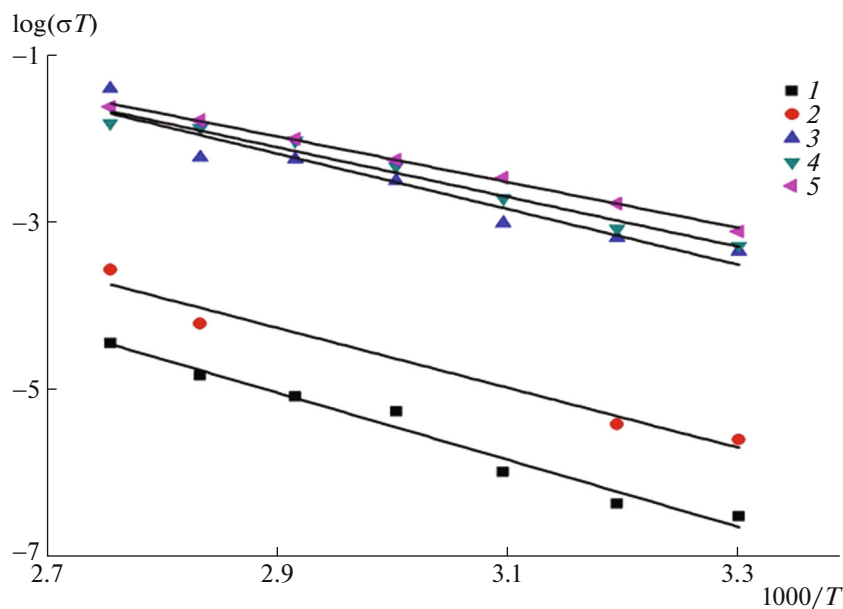
Fig. 5. (Color online) Temperature dependent behavior of PEO/PVP/lithium acetate polymer electrolytes: (*1*) 0, (*2*) 5, (*3*) 10, (*4*) 15, and (*5*) 20 wt % lithium acetate.

Dielectric Studies

The dielectric constant of the polymer blends with different concentrations of lithium acetate is denoted in Figs. 7a and 7b.

The complex dielectric constant of a system is defined by,

$$\varepsilon^* = \varepsilon' - j\varepsilon'', \qquad (3)$$

where ε' and ε'' denotes the real (dielectric permittivity) and imaginary (dielectric loss) part of dielectric constant.

Figure 7a illustrates the deviation of the dielectric permittivity ε through frequency for the PEO/PVP/20 wt % lithium acetate polymer electrolyte at different temperatures. The plot obtained for

Table 2. Conductivity and activation energy of PEO/PVP/lithium acetate solid polymer electrolytes

Composition	Conductivity, S/cm	Activation energy, eV
PEO/PVP	1.01×10^{-9}	0.76
PEO/PVP/5% lithium acetate	8.36×10^{-9}	0.67
PEO/PVP/10% lithium acetate	1.47×10^{-6}	0.62
PEO/PVP/15% lithium acetate	1.72×10^{-6}	0.56
PEO/PVP/20% lithium acetate	2.56×10^{-6}	0.51

dielectric permittivity denotes the monotonic diminish in the permittivity with low frequencies and achieves a steady rate at higher frequencies [39–45]. However by raising the electric field, the dipoles in the polymer electrolytes are not having the capacity to take after the field variations at high frequencies and there is an impact due to the electrode polarization. The dielectric permittivity begins to go down [47]. The occasional inversion of the field happens so quick at higher frequencies and there is an absence of over abundance ion dissemination towards the field.

Argand Plot Analysis

The Argand plot analysis gives the nature of relaxation processes present in the polymer electrolytes at different temperatures. Figure 8 shows the Argand plot of 20 wt % lithium acetate doped PEO/PVP polymer matrix at different temperature. The figure shows incomplete semicircle which explains the non Debye nature of the polymer electrolytes. So that two relaxation processes occur in polymer electrolytes. One is due to the dipolar relaxation and the other is occurred because of the existence of permanent dipoles on the side chains of the polymer backbone. The existence of relaxation time is because of the hopping of ions, space charge polarization and inhomogenetic of the material [48]. The semicircle with diameter below the axis indicates that the motion of ions and the polymer segmental motion are strongly coupled. The radius of the arc in the Argand plot is highly related to the electrical conductivity. The larger arc relates to the lower conductivity [49].

Tangent Spectra Analysis

Dissipation of energy takes place during the ionic transport and polarization of a dipole and it can be explained by the tangent loss. The morphology of the polymer, crystallinity level and molecular weight are
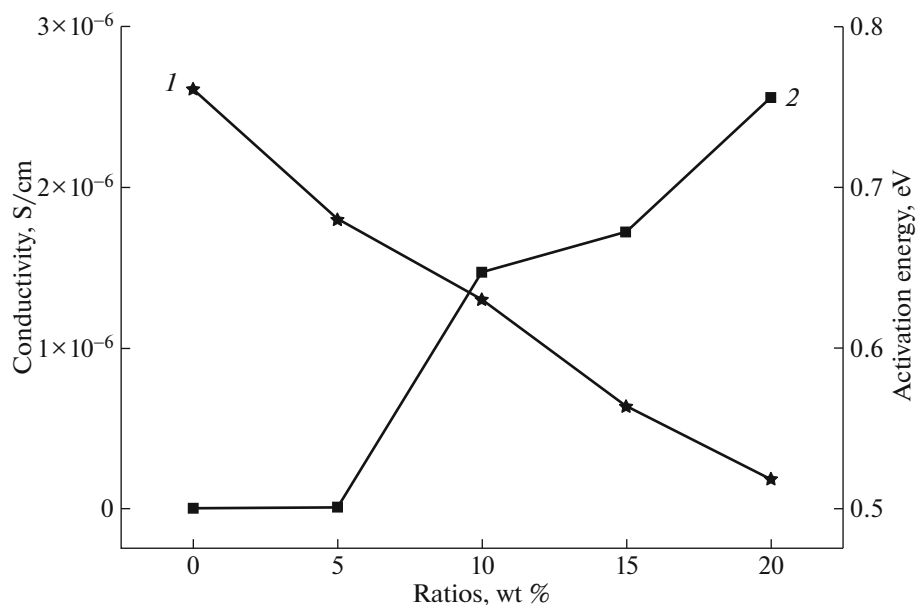
Fig. 6. Salt concentration (*1*) vs. activation energy and (*2*) vs. conductivity.
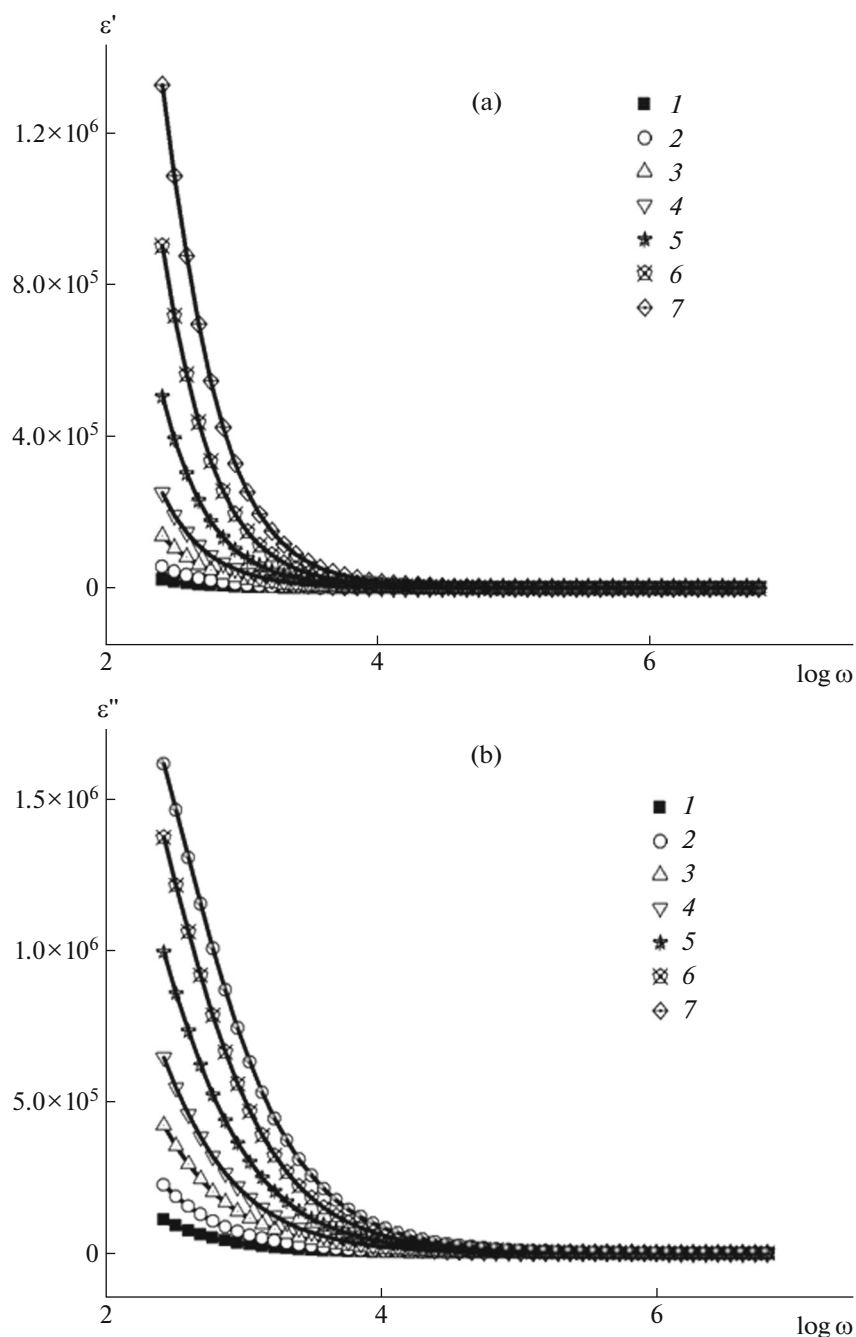
Fig. 7. (a) Dielectric constant and (b) dielectric loss for PEO/PVP/6 wt % lithium acetate at different temperatures: (*1*) 303, (*2*) 313, (*3*) 323, (*4*) 333, (*5*) 343, (*6*) 353, and (*7*) 363 K.

the influencing factors of loss tangent or dissipation factor. In Fig. 9a, the peak in the loss tangent plot demonstrates the event of phase transition when the temperature changes. From the XRD, it is clear that the intensity of PEO peak declines by increasing lithium acetate concentration and further-more the expansion in amorphous nature.

In Fig. 9b, the peaks observed tends to move in the direction of the higher frequency region with the rise

in temperature that move ahead to decrease in relaxation time of polymer systems. The swiftness of the polymer chain segmental motion motivates the amorphous nature of the polymer blend electrolytes while rising the temperature [48]. In this figure, it is observed that all the scaled tangent loss spectrum disintegrate into a single curve. Thus, dissipation of energy is temperature independent. From this, the scaling property of the tangent spectra is determined
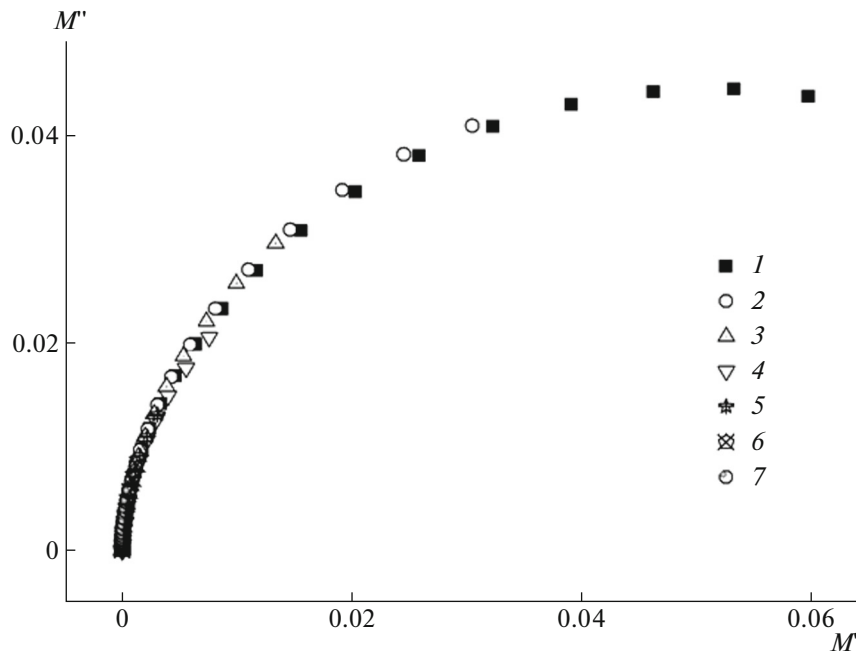
Fig. 8. Argand plot analysis of 20 wt % of lithium acetate doped PEO/PVP polymer blend electrolyte at different temperature: (*1*) 303, (*2*) 313, (*3*) 323, (*4*) 333, (*5*) 343, (*6*) 353, and (*7*) 363 K.

from the potency of the Coulomb interaction between movable particles. The relaxation frequency and the relaxation time of the prepared blend polymer electrolytes are presented in the Table 3.

Transference Number Studies

For the characterization of polymer electrolyte materials, transference number is considered as the utmost significant parameter. The transference number is used to relate the dispersion phenomena to the conductivity behavior of prepared polymer electrolytes. Wagner's polarizing technique is used to determine the Transference number [49]. In this method, the prepared polymer electrolyte is sandwiched between the two silver electrodes. By applying the fixed dc voltage (1.5 V) and observing the value of current by increasing the time, the transference number can be calculated.

The current consequently begins decreasing with time. The cell gets polarized by the passage of ions due to the electric field and thereby introduces a concentration gradient. Electrons or holes then only convey the polarization current. The transference numbers t_{ele} and t_{ion} are computed by the equations.

$$t_{ion} = (I_t - I_e)/I_i, \qquad (4)$$

Figure 10 denotes the graph between the polarization current versus time for different polymer electrolytes. From Table 4, transference number of polymer electrolytes are in the range of 0.86–0.96. From this, it is confirmed that the charge transport of the investigated polymer electrolytes is predominately due to ions.

The electron contribution is highly negligible in all the samples as suggested by the other workers [50, 51]. The transference number (t_{ion}) of the prepared polymer electrolyte films is closed by unity and denotes the conductivity is mainly due to lithium ions. So that, these kinds of polymer electrolytes are appropriate for solid-state electrochemical cells applications.

M.V. Leena Chandra, reported that charge carrier of the prepared polymer electrolytes are calculated using the following equation [54]:

$$n = N_A \rho x \text{ (molar ratio of the} \atop \text{salt/molecular weight of the salt)}, \qquad (5)$$

where N_A—Avogadro's number, ρ—density of the salt.

Table 3. Relaxation time for 20 wt % of lithium acetate with PEO/PVP polymer blend at various temperatures

Temperature, K	Hopping frequency ω	Relaxation time τ
303	24 322	4.11×10^{-5}
313	55 335	1.80×10^{-5}
323	102 565	9.74×10^{-5}
333	147 570	6.77×10^{-6}
343	259 417	3.85×10^{-6}
353	457 088	2.18×10^{-6}
363	920 449	1.08×10^{-6}
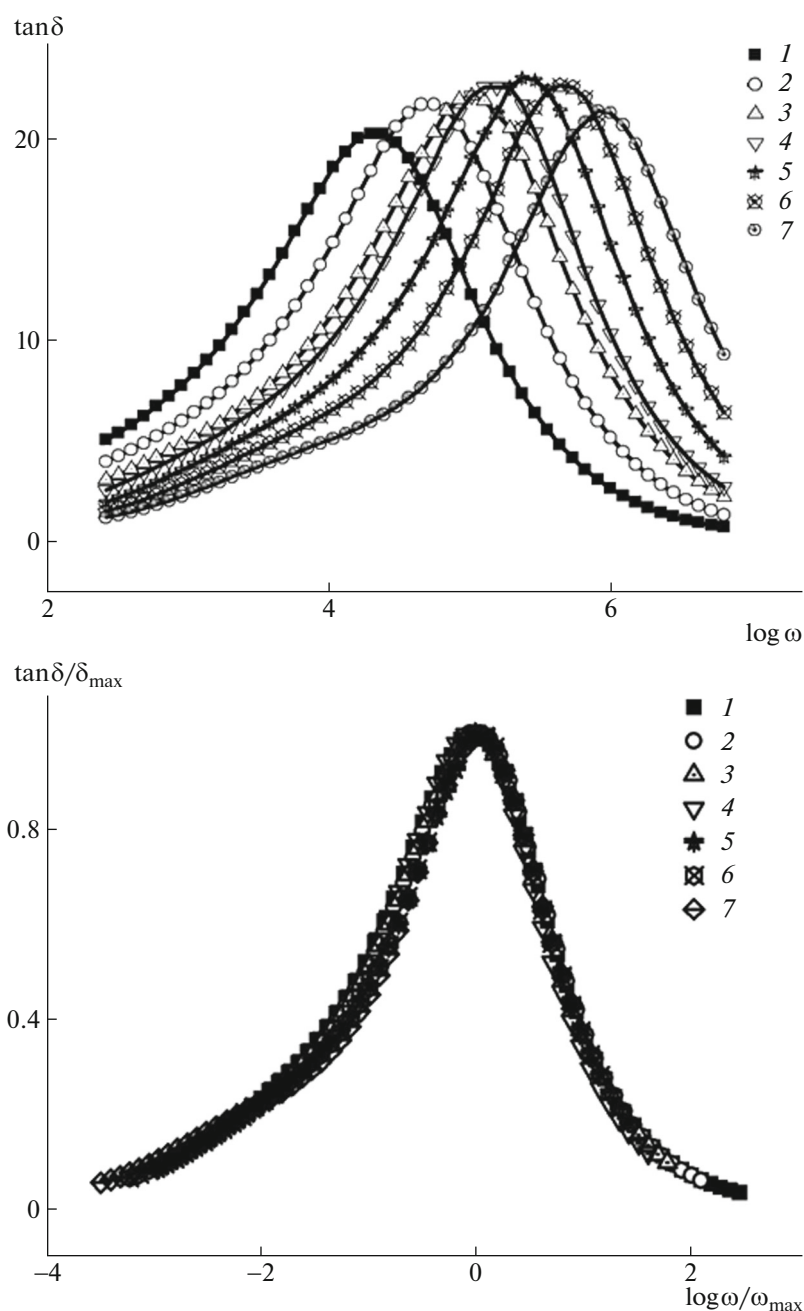
Fig. 9. (a) Tangent analysis and (b) tangent master curve of PEO/PVP/20 wt % of lithium acetate at different temperatures: (*1*) 303, (*2*) 313, (*3*) 323, (*4*) 333, (*5*) 343, (*6*) 353, and (*7*) 363 K.

Table 4. Transference numbers, mobility and carrier concentration of different wt % of lithium acetate with PEO/PVP polymer blend

Composition	Transference number t_{ion}	t_{ele}	D_+, cm^2/s	D_-, cm^2/s	μ_+, cm^2/(V s)	μ_-, cm^2/(V s)
PEO/PVP	0.95	0.05	—	—	—	—
PEO/PVP/5% lithium acetate	0.86	0.14	3.05×10^{-12}	4.97×10^{-13}	1.17×10^{-10}	1.9×10^{-11}
PEO/PVP/10% lithium acetate	0.94	0.06	2.93×10^{-10}	1.87×10^{-11}	1.12×10^{-08}	7.17×10^{-10}
PEO/PVP/15% lithium acetate	0.95	0.05	2.31×10^{-10}	1.22×10^{-11}	8.86×10^{-09}	4.66×10^{-10}
PEO/PVP/20% lithium acetate	0.96	0.04	2.61×10^{-10}	1.09×10^{-11}	9.99×10^{-09}	4.16×10^{-10}
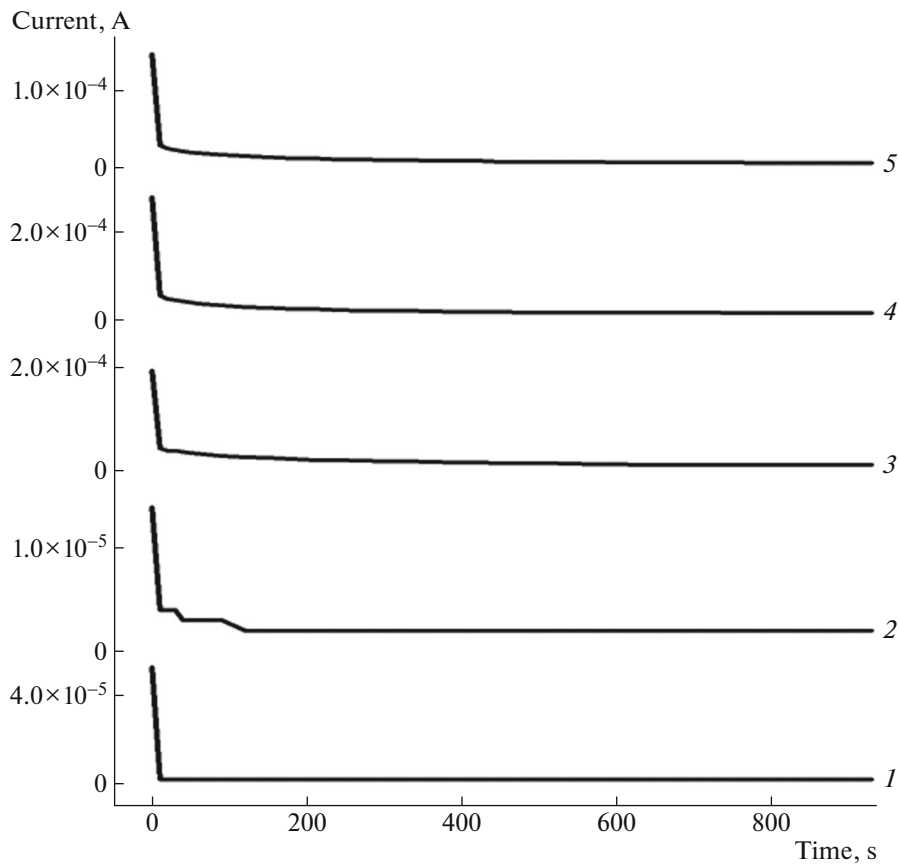
Fig. 10. Current vs. time for various wt % lithium acetate based PEO/PVP polymer electrolytes: (*1*) 0, (*2*) 5, (*3*) 10, (*4*) 15, and (*5*) 20% lithium acetate.

From the charge carrier and transference number, diffusion coefficient and mobility of both anion and cations are calculated by the following formula by Arof et al. [30]:

$$D = D_+ + D_- = KT\sigma/ne^2, \qquad (6)$$

and

$$\mu = \mu_+ + \mu_- = \sigma/ne, \qquad (7)$$

Charge carrier and carrier concentration and mobility of both anion and cations are tabulated in Table 4.

CONCLUSIONS

PEO/PVP/lithium acetate polymer membranes are prepared in different compositions. In the X-ray spectrum, there is a decrease in the peaks corresponding to PEO by increasing the lithium acetate concentration. The increase in the amorphous nature point out the absolute dissolution of the salt with the blend polymer matrix. The complexation between the polymer and the salt is confirmed by the FTIR spectroscopic analysis. There exists an ever-changing bands by changing the concentration of salt. The conductivity of the polymer blend electrolytes improved by increasing the concentration of lithium acetate as well as temperature. The blend polymer electrolyte PEO/PVP/20 wt % lithium acetate is having the higher conductivity as 2.56×10^{-6} S/cm. From the dielectric analysis, obviously the dielectric consistent and loss diminishes monotonically with expanding frequency and accomplishes a steady value at higher frequencies. The field variation is coupled with the creation of electric dipoles. From the tangent plot, the variation of temperature shifts the peaks towards the higher frequencies and thereby diminish the relaxation time. The acquired transference number for the prepared polymer blend electrolytes are in the range of 0.86−0.96 which means that the conductivity is fundamentally because of ions. Thus the prepared polymer electrolytes can be employed for electrochemical applications.

REFERENCES

1. S. Ramesh, G. B. The, R.-F. Louh, Y. K. Hou, P. Y. Sin, and L. J. Yi, Ind. Acad. Sci. **35**, 87 (2010).

2. P. Santhosh, T. Vasudevan, A. Gopalan, and K. P. Lee, J. Power Sources **160**, 609 (2006).

3. S. Rajendran, R. Kannan, and O. Mahendran, Mater Lett. **49**, 172 (2001).

4. M. Sundar and S. Selladurai, Ionics **12**, 281 (2006).

5. F. M. Gray, *Solid Polymer Electrolytes* (VCH, New York, 1991).

6. D. E. Fenton, J. M. Parker, and P. V. Wright, Polymer **14**, 589 (1973).

7. K. Kesavan, C. M. Mathew, S. Rajendran, C. Subbu, and M. Ulaganathan, Braz. J. Phys. **45**, 19 (2015).

8. M. Kovac, M. Gaberscek, and J. Grdadolnik, Electrochim. Acta **44**, 863 (1998).

9. A. Ghosh and P. Kofinas, ECS Trans. **11**, 131 (2008).

10. Z. Ahmad, N. A. Al-Awadi, and F. Al-Sagheer, Polym. Degrad. Stab. **92**, 1025 (2007).

11. P. G. Bruce, *Solid State Electrochemistry* (Cambridge University Press, Cambridge, 1995), p. 344.

12. Y. G. Andreev and P. G. Bruce, Electrochim. Acta **45**, 1417 (2000).

13. D. A. J. Rand, J. Power Sources **4**, 1 (1979).

14. K. KiranKumar, M. Ravi, Y. Pavani, S. Bhavani, A. K. Sharma, and V. V. R. Narasimha Rao, Phys. B (Amsterdam, Neth.) **406**, 1706 (2011).

15. J. J. Zieba, Y. Zhang, and P. N. Prasad, Sol-Gel Opt. II **1758**, 287 (1992).

16. H.-D. Wu, I.-D. Wu, and F.-C. Chang, Polymer **42**, 555 (2001).

17. B. K. Money, PhD Thesis (IIT Madras, Madras, 2019).

18. P. Knauth, Solid State Ionics **180**, 911 (2009).

19. *Lithium Batteries-Science and Technology,* Ed. by G. Nazri and G. Pistoia (Kluwer Acad. Publ., London, 2004).

20. A. M. Abdelghany, M. S. Meikhail, and H. Y. Salah, Res. J. Pharm., Biol. Chem. Sci. **6** (1), 1352 (2015).

21. B. L. Papke, M. A. Ratner, and D. F. Shriver, J. Electrochem. Soc. **129**, 1434 (1982).

22. I. Sireerat, PhD Thesis (School Chem. Inst. Sci., Suranaree Univ. Technol., Suranari, 2005), pp. 54–175.

23. C. V. Subba Reddy, A.-P. Ji, Q.-Y. Zhu, L.-Q. Mai, and W. Chen, Eur. Phys. J. E: Soft Matter Biol. Phys. **19**, 471 (2006).

24. S. Ramesh and A. K. Arof, Mater. Sci. Eng., B **85**, 11 (2001).

25. N. Ammakutti Sridevi, K. Karuppasamy, S. Balakumar, and X. Sahaya Shajan, Chem. Sci. Trans. **1**, 311 (2012).

26. O. Borodin, G. D. Smith, R. Bandyopadhyaya, P. Redfern, and L. A. Curtiss, Model. Simul. Mater. Sci. Eng. **12**, S73 (2004).

27. M. R. Johan and L. M. Ting, Int. J. Electrochem. Sci. **6**, 4737 (2011).

28. J. M. G. Cowie, in *Polymer Electrolyte Reviews,* Ed. by J. R. Mac Callum and C. A. Vincent (Elsevier Appl. Sci., London, 1987), Vol. 1, p. 92.

29. B. Tareev, *Physics of the Dielectric Materials* (MIR Publications, Moscow, 1979) [in Russian].

30. S. Ramesh, A. H. Yahana, and A. K. Arof, Solid State Ionics **152**, 291 (2002).

31. P. C. K. Pillai, P. Khurana, and A. Trilatera, Mater. Sci. Lett. **5**, 629 (1986).

32. A. A. Mohamad, N. S. Mohamad, M. Z. A Yahya, R. Othman, S. Ramesh, Y. Alias, and A. K. Aroof, Solid State Ionics **156**, 171 (2003).

33. S. Selvasekarapandian, R. Baskaran, and M. Hema, Phys. B (Amsterdam, Neth.) **357**, 412 (2005).

34. S. Rajendran, R. S. Babu, and M. Usha Rani, Bull. Mater. Sci. **34**, 1525 (2011).

35. R. Damle, P. N. Kulkarni, and S. V. Bhat, Ind. Acad. Sci. **72**, 555 (2009).

36. M. Tripathi, S. Trivedi, R. Dhar, M. Singh, N. D. Pandey, and S. L. Agrawal, Phase Transitions **84**, 11 (2011).

37. W. Wang and P. Alexandridis, Polymers **8**, 387 (2016).

38. N. Ahad, E. Saion, and E. Gharibshahi, J. Nanomater. **2012**, 857569 (2012).

39. L. N. Shukla, A. K. Thakur, A. Shukla, and D. T. Marx, Int. J. Electrochem. Sci. **9**, 7644 (2014).

40. H. G. L. Coster, T. C. Chilcott, and A. C. F. Coster, Bioelectrochem. Bioenerg. **40**, 79 (1996).

41. H. S. Tewari and A. Pati, Int. J. Recent Adv. Phys. **2**, 4 (2013).

42. A. Manjunath, T. Deepa, N. K. Supreetha, and M. Irfan, Adv. Mater. Phys. Chem. **5**, 295 (2015).

43. S. Badr, E. Sheha, R. M. Bayomi, and M. G. El-Shaarawy, Ionics **16**, 269 (2010).

44. S. K. Tripathi, A. Gupta, and M. Kumar, Bull. Mater. Sci. **35**, 969 (2012).

45. A. Arya, S. Sharma, A. L. Sharma, D. Kumar, and M. Sadiq, Asian J. Eng. Appl. Technol. **5**, 4 (2016).

46. A. Islam, Z. Imran, T. Yasin, N. Gull, S. M. Khan, M. Shafiq, A. Sabir, M. A.Munawar, M. H. Raza, and T. Jamil, Mater. Res. **18** (6), 1256 (2015).

47. B. Chatterjee, N. Kulshrestha, and P. N. Gupta, Int. J. Eng. Res. Ind. Appl. **5** (6), 116 (2015).

48. K. C. Kwan, *Dielectric Phenomena in Solids* (Elsevier, New York. 2004).

49. E. S. Matveeva, Synth. Met. **79**,127 (1996).

50. Merhawi Abreha Gebreyesus, Y. Purushotham, and J. Siva Kumar, Heliyon **2** (7), e00134 (2016).

51. A. K. Joncher, Mater. Sci. **13**, 553 (1987).

52. P. B. Bhargav, V. M. Mohan, A. K. Sharma, and V. V. R. N. Rao, Curr. Appl. Phys. **9**, 165 (2009).

53. K. Funke, B. Roling, and M. Lange, Solid State Ionics **105**, 195 (1998).

54. M. V. Leena Chandra, S. Karthikeyan, S. Selvasekarapandian, D. Vinoth Pandi, S. Monisha, and S. Arulmozhi Packiaseeli, Ionics **22**, 2409 (2016).